Volume Recovery near the Glass Transition Temperature in Poly(vinyl acetate): Predictions of a Coupling Model

R. W. Rendell,*† K. L. Ngai, and G. R. Fong†

Naval Research Laboratory, Washington, D.C. 20375-5000

J. J. Aklonis

Department of Chemistry, University of Southern California, Los Angeles, California 90089-1062. *Received July 16, 1986*

ABSTRACT: Time-dependent volume changes following an increasing temperature jump are known to exhibit an anomaly as the equilibrium volume is approached. Small differences in initial temperature result in large differences in the rate of change of volume deviation δ near $\delta = 10^{-4}$. Kovacs' $\tau_{eff} \equiv -\delta(d\delta/dt)^{-1}$ plots exhibit this as a "gap" between the curves, which has not previously been explained. We show that the coupling model of relaxation is able to produce the gap. The τ_{eff} curves, including the size of the gap, are accurately reproduced. The size of the gap is used to predict the Kohlrausch exponent n for relaxation at equilibrium, and this is found to agree with shear measurements of Plazek. Furthermore, the shapes of the τ_{eff} plots are used to predict the δ dependence of the shift factor. The predicted shift factor agrees with the Doolittle equation obtained by Kovacs, Stratton, and Ferry at 35 °C and crosses over to the Doolittle equation of Williams and Ferry at 40 °C. Finally, a single primitive molecular relaxation time predicted by the coupling model is shown to account for the terminal dispersion, the softening dispersion, and the volume recovery in poly(vinyl acetate).

1. Introduction

A model of relaxation (referred to here as the "coupling model") has been recently developed and applied to problems in glasses, polymers, and other complex systems.[1-3] It is a model that incorporates generic properties of dynamical systems in a calculation of relaxation. The result is a kinetic equation that has a time-dependent rate in contrast to the more conventionally considered time-independent rates. Application of the coupling model has produced many verified predictions and resolved apparent anomalies in various fields that presently have no alternate explanation. In this work we examine volume recovery of poly(vinyl acetate) (PVAc) using the coupling model. However, before describing the details of the coupling model and its implications for the structural recovery of glass, let us briefly review the phenomena of volume recovery and some current formalisms used to describe it.

Liquids and polymers cooled or heated in the vicinity of the glass transition temperature T_g are found to be out of structural equilibrium when the rate of cooling or heating exceeds the rate of structural (molecular) rearrangements. The subsequent structural recovery of the glass has been extensively studied experimentally by many groups by following the time dependence of quantities such as volume, enthalpy, refractive index, or density fluctuations. The observed recovery in glassy materials shows common behavior: (i) nonlinearity with respect to the magnitude of departure from equilibrium, (ii) asymmetry with respect to the sign of the departure, and (iii) memory effects that are sensitive to the thermal and physical aging history.

An important example of this type of study is the measurements of isothermal volume recovery following a single rapid temperature change obtained by Kovacs.[4,5] This work was carried out on PVAc, polystyrene, and glucose and is notable for the quality and thoroughness of the data. The samples were subjected to a standard thermal pretreatment that included annealing to erase previous history. Samples in volume equilibrium at an initial temperature of T_0 were rapidly heated or cooled in the dilatometer to a final temperature of T_1. Thermal equilibrium is reached in less than 2 min while the approach to volume equilibrium generally takes several hours. The departure from volume equilibrium can be defined in terms of the dimensionless variable δ

$$\delta \equiv (v - v_\infty)/v_\infty \tag{1.1}$$

where v is the instantaneous specific volume and v_∞ is its equilibrium value at the same temperature (and pressure).

Figure 1a shows measured values of δ for PVAc. The upper curve shows contraction where the sample has been rapidly cooled from $T_0 = 40$ °C to $T_1 = 35$ °C and the approach to equilibrium involves positive values of δ. The lower curve shows expansion, $\delta < 0$, after a rapid temperature increase from $T_0 = 30$ °C to $T_1 = 35$ °C. The asymmetry between expansion and contraction is clear from this figure. A very sensitive parameter called τ-effective (τ_{eff}) was first introduced by Kovacs[5] and is defined by

$$\tau_{eff}^{-1} \equiv -\delta^{-1}(d\delta/dt) \tag{1.2}$$

This can be determined from the data in Figure 1a, and a plot of the corresponding τ_{eff} is shown in Figure 1b. Curves corresponding to other values of T_0 have also been included. The τ_{eff} representation is quite sensitive to the approach in time to equilibrium, and it is able to reveal many characteristics that are not easily seen from the primary data. Figure 1 shows only a portion of Kovacs' data on PVAc, but the richness of the behavior is evident.

The complex behavior shown by the δ and τ_{eff} plots of the volume recovery data have been used as proving grounds for an understanding of glassy behavior. Phenomenological models, which can reproduce many of the essential features shown in Figure 1 have been previously developed. These models contain two elements that seem necessary to understand this behavior: (i) a broad relaxation spectrum and (ii) a dependence of the relaxation time(s) on structure (i.e., δ) as well as temperature. The Kovacs, Aklonis, Hutchinson, and Ramos (KAHR) multiparameter model[6] splits up the total departure from equilibrium δ into N individual contributions δ_i such that $\delta = \sum\delta_i$. The decay of each δ_i is governed by a relaxation

† Sachs/Freeman Associate.

0024-9297/87/2220-1070$01.50/0

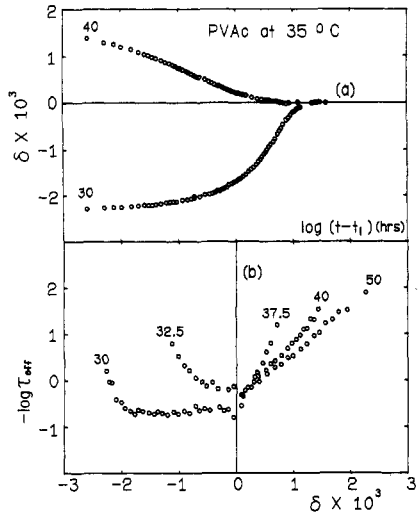

Figure 1. Volume recovery data of Kovacs (ref 5) in PVAc at 35 °C: (a) volume deviation (δ, eq 1.1) vs. time; (b) $-\log \tau_{eff}$ (eq 1.2) vs. δ.

time τ_i which is a function of the total δ as well as temperature

$$\frac{d\delta_i}{dt} = -\tau_i^{-1}\delta_i \tag{1.3}$$

Therefore

$$\delta = \delta_0 \sum^{N} g_i \exp\left[-\int_0^t dt'\,\tau_i^{-1}\right] \tag{1.4}$$

$$\tau_i = \tau_i(T,\delta) \tag{1.5}$$

The normalization condition $\sum g_i = 1$ ensures that $\delta(0) = \delta_0$ where $\delta_0 = \Delta\alpha(T_0 - T_1)$ and $\Delta\alpha$ is the excess expansion coefficient of the liquid with respect to the glass. For PVAc, $\Delta\alpha \cong (4\text{–}5) \times 10^{-4}$ K^{-1}. This partitioning of the response among various modes that have different relaxation times is analogous to the distribution of relaxation times that has often been invoked to interpret linear viscoelastic experiments. However, in the present case, each of the relaxation times should be dependent on the molecular motions in the system, and this dependence is measured by the total δ as in eq 1.5. This physical requirement on the relaxation times means that eq 1.4 for the time evolution of δ must be solved self-consistently in δ. This self-consistent modification of the τ_i as δ evolves allows the model to exhibit asymmetry and nonlinearity behavior as observed.

In practice, application of the KAHR model is usually done with T and δ dependences of τ_i factorized as

$$\tau_i(T,\delta) = \tau_{ir} a_T a_\delta \tag{1.6}$$

with empirical expressions used for the shift factors a_T and a_δ. An example of a form often used for these shift factors is

$$a_T a_\delta = \exp[-\theta(T - T_r)] \exp[-(1 - x)\theta\delta/\Delta\alpha] \tag{1.7}$$

where θ and x are material-dependent parameters and T_r is a reference temperature. Equation 1.7 has been shown to be equivalent to several other empirical expressions commonly used, including the Doolittle equation, at least within a narrow range of temperature.[7] Empirical expressions such as these have been proposed by several workers as generalizations of equilibrium shift factors to structural nonequilibrium situations. The parameter θ can be estimated from the apparent activation energy controlling the rate of configurational rearrangements, and the parameter x is adjustable. The T and δ dependences are assumed to be the same for each mode but the value of the prefactor τ_{ir} is spread over several decades in time corresponding to $i = 1, ..., N$.

Although asymmetry and nonlinearity behavior are exhibited even by a single-parameter KAHR model (i.e., $N = 1$), a broad distribution of many relaxation times is required to produce an approximation to the detailed shapes in Figure 1. Multiple relaxation times in the KAHR model are also required to reproduce memory effects that are observed in experiments with multiple temperature jumps. The distribution of relaxation times can be specified by giving the weights, g_i, corresponding to each τ_i in eq 1.4. By testing many different distributions, it can be determined what distribution is required to produce the features of Figure 1. This leads to a distribution $g_i(\tau_i)$ that essentially consists of two parts: a long-time section spanning about 2 decades of time and containing about 90% of the weight and a short-time tail spanning about 3 decades of time. The number of τ_is required for a reasonable description of Figure 1 is about 50. This spectrum takes the approximate shape of "two boxes", although the shapes of the boxes have been smoothed in some fits to the data.[7] The short-time tail piece is required to produce the upturn of the expansion τ_{eff} curves at short times in Figure 1 while the slopes of the τ_{eff} curves are sensitive to the width of each piece of the spectrum. The values of the g_i are assumed to be independent of δ and T so that the entire distribution shifts rigidly along the logarithmic time scale by an amount $\log (a_T a_\delta)$ when δ or T vary. The qualitative behavior of Figure 1 can be interpreted[8] within the KAHR model in terms of the change in overlap between this shifting distribution and the decay function $\exp[-\int_0^t dt'\,\tau^{-1}]$ of eq 1.4. As we discuss below, however, there are some features of the data that cannot be reproduced by the KAHR model.

Relaxation spectra from equilibrium experiments for quantities such as the relaxation modulus have also been formally decomposed into a distribution of relaxation times that roughly has a long-time piece of large weight and a short-time tail. The shape of the corresponding relaxation decay functions can often be accurately described by the fractional exponential or Kohlrausch function

$$\phi(t) = \exp[-(t/\tau)^{1-n}] \tag{1.8}$$

It has been pointed out by KAHR[6] that a relaxation function of the form $\phi(t) = \sum g_i \exp(-t/\tau_i)$ where $g_i(\tau_i)$ is a two-box distribution of the type above is similar to the Kohlrausch function eq 1.8 for a particular value of n. Equation 1.4 would approximate such a form at equilibrium where each τ_i is simply a constant. Matsuoka et al.[27] have recently discussed many aspects of the relaxation spectra within the KAHR model.

Other models have been developed that have the same essential features as the KAHR model. Robertson's model[9-13] also has a distribution of structurally dependent relaxation times. However, the model attempts to relate the relaxation times to a distribution of free volume. The rate of change of free volume from a local region in the glass is assumed to depend on the average free volume in that region. The free volumes are taken to correspond to conformational rearrangements within a simple model of cis and trans backbone rotational states. For simplicity, the free volume is restricted to a set of N discrete values, and these free volume values are distributed according to a binomial distribution. The variance of this distribution is estimated[10,12] from the formula for equilibrium thermal density fluctuations, $\Delta\kappa kT/V$, where $\Delta\kappa$ is the difference between compressibilities of liquid and glass and V is the

volume governing a conformational transformation. For PVAc, Robertson argues that $V \cong 3.2$ nm^3 or larger and that fluctuations on this scale are important. However, this is inconsistent with experimental SAXS measurements.[23,14] The rates at which the volume element gains or loses free volume are assumed to be governed by a WLF equation in terms of the average free volume in V and a number (e.g., 12 for hexagonal closest packing) of neighboring regions. The WLF form of the rates is supplemented by a prefactor that has an Arrhenius dependence on temperature. In terms of these rates, Robertson then constructs an equation for the probability $\omega_j(t)$ that a region contains free volume value f_j at time t. The average free volume at time t is then $\bar{f} = \sum_{j=1}^{N} f_j \omega_j(t)$. With a relation assumed between free volume and the actual volume deviation, $d\delta/dt = (d\bar{f}/dt)(\bar{f} - \bar{f}_{eq})^{-1}$, the result for δ takes the form

$$\delta(t) = \delta_0 \sum_{i=1}^{N} g_i \exp[-t/\tau_i] \tag{1.9}$$

The τ_i^{-1} are the magnitudes of the nonzero eigenvalues of a matrix of the transition rates between the free volume values. The weighting factors g_i determine the shape of the relaxation spectrum. In the application of Robertson's model to Kovacs' volume recovery data, the spectrum is found to be similar to that assumed by KAHR in that it has a breadth many decades wide and more highly weighted at the long-time end.[12,13] However, each spectral line is weighted according to the remaining deviation from equilibrium of the free volume state giving rise to the line, and, unlike the KAHR model, the spectrum can change shape as the volume recovery proceeds.[13] However the spectrum is predicted to narrow following a jump down in temperature, contrary to experimental data.[42,14] Equation 1.9 takes the form of a sum of decaying exponentials in time rather than a sum of exponentials of an integral over the relaxation times as in the KAHR model eq 1.4. This difference arises because Robertson assumed that the transition rates do not change over moderate time intervals. He found that the average free volume (and the rates that depend on it) need only be reevaluated intermittently, and that this does not introduce significant error. In spite of differences in detail and problems with its physical basis, Robertson's equation for the volume recovery has many of the same basic features as the KAHR model. Robertson's model does exhibit some of the features of Figure 1; however, as we shall show, it fails to reproduce some important aspects of the data.

Moynihan and co-workers[15] have also introduced a phenomenological model for structural recovery that has a broad relaxation spectrum and structurally dependent relaxation times. However, instead of a weighted sum of exponentials, as in the KAHR and Robertson models, Moynihan uses a single relaxation function that is intrinsically nonexponential. For volume recovery following a single temperature jump this can be written

$$\delta(t) = \delta_0 \exp\left[-\left(\int_0^t dt'\, \tau^{-1}\right)^{\beta}\right] \tag{1.10}$$

where $\tau \equiv \tau(T,\delta)$ and $0 < \beta < 1$. The parameter β produces a broad effective relaxation spectrum even though there is only a single relaxation time τ. Equation 1.10 was not derived but was simply proposed by Moynihan as an attempt to generalize the empirical Kohlrausch function eq 1.8 to situations of structural nonequilibrium. Since β is constant, the effective relaxation spectrum does not change shape but shifts rigidly with τ as in the KAHR model. In practice, Moynihan et al. have used an empirical expression for $\tau(T,\delta)$ first introduced by Narayanaswamy[16]

$$\tau(T,\delta) = A \exp\left[\frac{x\Delta h}{RT} + \frac{(1-x)\Delta h}{RT_f}\right] \tag{1.11}$$

where A, x, Δh are adjustable constants and the fictive temperature, T_f, is given by $\delta = \Delta\alpha(T_f - T)$. KAHR have pointed out that eq 1.11 is equivalent to eq 1.7 within a narrow range of temperature.[7] As with KAHR and Robertson, the Moynihan model can exhibit many of the features of Figure 1. The applications of the Moynihan model have been extended and studied by several groups.[17-19]

Although the KAHR, Robertson, and Moynihan models have attained degrees of success in reproducing the features of Figure 1, some serious problems remain. The most prominent discrepancy is the inability of any of these models to even qualitatively reproduce the expansion ($\delta < 0$) data as δ approaches zero. In Figure 1, the values of $-\log \tau_{eff}$ corresponding to $T_0 = 30$ and 32.5 °C differ by about half a decade near $\delta = 10^{-4}$ (the expansion "gap"). The volume deviation measurements near $\delta = 10^{-4}$ are known to an accuracy of $\pm 10^{-5}$. We quote Kovacs:[4] "Nous avons pu estimer ainsi des variations de volume à $\pm 10^{-5}$ près et les densités à $\pm 10^{-4}$ g/cm^3 près". The result involves differences that are much greater than experimental error and the gap is, therefore, a real effect. This effect is also observed in expansion measurements in PVAc at different T_1 values as well as in other materials such as polystyrene[20] and zinc chloride glass.[21] In contrast, the contraction ($\delta > 0$) data appear to converge for small δ. This situation has prompted discussion in the literature concerning whether the limiting state that the annealed glass approaches is a true equilibrium state, the sensitivity of volume as an indicator of equilibrium, the differences in relaxation times of different relaxing quantities, and related questions.[22-25] However, the problem has remained unresolved.

The τ_{eff} plots for the contraction data are relatively featureless and have roughly a constant slope at each T_0. This is reproduced by the KAHR, Robertson, and Moynihan models. In particular, the KAHR model is able to closely fit this data by using a smoothed two-box distribution.[7] For $T_0 \gtrsim 40$ °C the assumption of an instantaneous quench from T_0 to T_1, which was assumed in eq 1.4, 1.9, and 1.10, is no longer a good approximation. At these higher temperatures, the relaxation times may be short enough that some recovery may already have occurred during the cooling ramp. The initial δ may then be smaller than $\delta_0 = \Delta\alpha(T_0 - T_1)$ at $T = T_1$. Some of the minor descrepancies between the models and the contraction data have been attributed to the necessity of introducing a finite cooling ramp, and this is certainly physically plausible.[7] The discrepancies with the expansion data are, however, more serious. The $-\log \tau_{eff}$ for the expansion data decrease rapidly and then turn over to a region that is roughly flat or may even have positive slope as δ approaches zero. The KAHR, Robertson, and Moynihan models exhibit this general behavior, but all the curves rapidly approach the same point on the $\delta = 0$ axis regardless of the value of T_0. Not only does this prevent a quantitative description of the expansion data but also the essential feature of a "gap" between the expansion curves is not even qualitatively reproduced.

As an example, we show in Figure 2 a calculation of τ_{eff} based on Moynihan's phenomenological expression eq 1.10. We have numerically solved eq 1.10 self-consistently in δ using an iterative procedure with $\beta = 0.5$, $\tau(35,0) = 0.59$ h and the dependence of the relaxation time on δ, $\tau(T,\delta)$

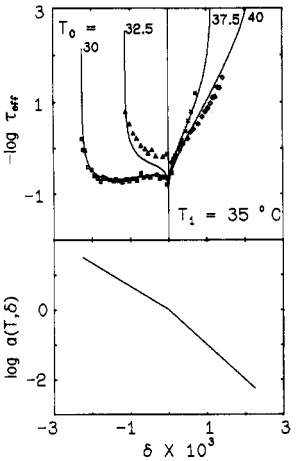

Figure 2. Comparison of Moynihan's phenomenological expression (eq 1.10) with the expansion data of Figure 1. Here β = 0.5, $\tau(35,0)$ = 0.59 h, $\Delta\alpha = 4.65 \times 10^{-4}$ K^{-1}, and $a(T,\delta) = \tau(T,\delta)/\tau(35,0)$ was adjusted for best fit as shown. The expansion gap cannot be reproduced for any choice of parameters.

$\equiv \tau(35,0)a(T,\delta)$, as shown in Figure 2. To allow the Moynihan expression as much flexibility as possible, the $a(T,\delta)$ dependence on δ was chosen to obtain the best fit to the data rather than use the empirical formula eq 1.11. Although Figure 2 is calculated from the Moynihan model, it is also representative of the type of reproduction of the features produced by the KAHR and Robertson models. In particular, the "gap" near $\delta = 0$ between the expansion curves is not reproduced. In fact, we have examined the Moynihan model for β values from near zero to near one and for a variety of $a(T,\delta)$ functional dependences on δ. We used $a(T,\delta)$ variations ranging from a constant $a(T,\delta)$ to a $a(T,\delta)$ which decreased by several decades as $\delta \to 0$. The expansion curves are always found to rapidly approach one another near $\delta = 0$, and no gap is ever formed. Similar results were found by Ng and Aklonis[25] for the KAHR model. They examined the effect of the shape of the distribution function $g_i(\tau_i)$ and the effect of the x parameter in eq 1.7 which determines the strength of the δ dependence of the τ_i. They concluded that the behavior of the τ_{eff} expansion curves near $\delta = 0$ could not be produced by the KAHR model for any reasonable set of parameters. Robertson has also pointed out that his free volume based model does not reproduce this feature.[10-13]

This situation is a major shortcoming of these models, and it has not been clear how to rectify the problem. This is due to the phenomenological nature of these models. They have demonstrated that many of the features of volume recovery can be obtained with simply a broad relaxation spectrum and structural-dependent relaxation times. However, all of the approaches make assumptions concerning the dependence of the relaxation times on T and δ and on the method for producing a broad relaxation spectrum. The physical interpretation of many of the parameters and functions are not understood. In Moynihan's model, the form of the relaxation function eq 1.10 was taken as an assumption and not derived from any kinetic or rate theory appropriate to glassy systems. Therefore, even to the extent that agreement is obtained between the model and data, it is difficult to evaluate the results in a physically meaningful way. In addition, when empirical expressions such as the Narayanswamy form eq 1.11 are used for $\tau(T,\delta)$, the values of the constants are found to take physically unacceptable values. Application of the Moynihan model to describe PVAc data using eq 1.11 requires[26] the values $A = 3.6 \times 10^{-98}$ s and Δh = 142 kcal/mol. This extremely small time scale and very large activation enthalpy do not have any physical interpretation. Any further modifications of the Moynihan model must be considered arbitrary.

The KAHR model uses a sum of N decaying contributions δ_i that have not yet been physically identified. Each of these contributions were assumed to obey the simple rate equation, eq 1.3. KAHR have not insisted on a particular physical interpretation for these contributions. Robertson also uses a sum of N decaying contributions, but he has gone further and proposed an interpretation of these contributions in terms of free volume fluctuations. These fluctuations are assumed to control the rates of conformational changes for a very simple model of cis and trans backbone rotational states. The concept of a distribution of free volume is phenomenological and does not have a fundamental basis. Free volume can be a useful concept, but it is well-known that predictions based on free volume sometimes fail. In the present situation, the concept of free volume fluctuations has been shown experimentally to be irrelevant on the scale of the primary segmental motions.[14,23]

In brief, the major problems with the present descriptions of volume recovery are the inability to reproduce the gap near $\delta = 0$ in the expansion data, the lack of physical interpretation of many of the parameters and formulas describing the dependence of the relaxation times on T and δ, and the lack of a fundamental basis for the rate equations used to include dynamics in the models. In this paper, we demonstrate that the coupling model is able to help clarify each of these problems. The coupling model is described in section 2. It incorporates generic properties of complex dynamical systems into a relaxation calculation. The result is a rate equation with a time-dependent relaxation rate. The form of this rate equation has been derived from fundamental properties of complex dynamical systems. This result produces a broad relaxation spectrum even for a single relaxation mode. However, this broad spectrum is not equivalent to a distribution of relaxation times. This has been previously applied successfully to many glass and polymer problems.[1-3,33-37]

The coupling model is applied to PVAc volume recovery in section 3. It produces a broad relaxation spectrum and a structural-dependent relaxation time, but it readily produces the gap near $\delta = 0$ in expansion data. The coupling parameter n governs the breadth and shape of the effective relaxation spectrum, and this can be determined from the size of the expansion gap. The values of n agree with equilibrium compliance measurements of Plazek on PVAc. Furthermore, the detailed shape of the τ_{eff} plots (including the gap) can be used to predict the T and δ dependence of the relaxation time. At T = 35 °C, these predictions agree with the Doolittle equation measured independently by Kovacs, Stratton, and Ferry and at T = 40 °C with the Doolittle equation measured by Williams and Ferry at higher temperatures. These results provide strong evidence for the coupling model mechanism in the structural recovery of glasses. The coupling model also predicts properties of the primitive relaxation time. This is also discussed, and it is shown that the same underlying primitive relaxation time governs the terminal regime, the softening regime, and the volume recovery experiments. A summary is given in section 4.

2. Coupling Model of Relaxation

Relaxations of a macroscopic variable such as volume, enthalpy, stress, polarization, electric field, etc., have been observed in appropriate condensed matter systems such as glasses, amorphous polymers, polymer melts, viscous liquids, ionic conductors, and amorphous semiconduc-

tors.[1-3] In the simpler condensed matter systems such as crystals and simple liquids, the decay in time of a macroscopic variable can often be described by a rate equation with a constant rate $W_0 = \tau_0^{-1}$

$$d\phi/dt = -\tau_0^{-1}\phi \tag{2.1}$$

This leads to an exponential decay

$$\phi(t) = \phi(0) \exp(-t/\tau_0) \tag{2.2}$$

The origin of a simple rate equation with constant rate from the underlying equations of motion of the microscopic molecular degrees of freedom was studied over 30 years ago by van Hove, Prigogine, and others.[29] The microscopic variables are described by a Hamiltonian that describes the kinetic and potential energies of all the molecules and bonds which make up the system. The time development of the coordinates and momenta of the variables are governed by Hamilton's classical equations of motion (if quantum effects are not important). The macroscopic variable is a function of these coordinates and momenta, and it thereby also evolves in time. This evolution in time of the macroscopic variable can be dissipative, even though the underlying equations of motion are not, if the system is coupled to a heat bath. The heat bath is made up of a large number of fast degrees of freedom that remain in thermal equilibrium while the macroscopic variable decays on a longer time scale. van Hove and Prigogine described conditions for which the evolution of the macroscopic variable can be approximated by a Hamiltonian system coupled to a heat bath. For the class of Hamiltonians they studied, they obtained the rate equation with constant rate eq 2.1 (or the associated master equation with constant transition rate). The value of τ_0 depends on the details of the Hamiltonian under consideration.

Since these earlier studies on the microscopic origin of rate equations, there has been a resurgence of interest in the dynamical properties of Hamiltonians. In the past 15 years, a large body of work has demonstrated that the dynamics of Hamiltonian systems exhibit certain generic features.[30,31] For instance, quantum Hamiltonians generically possess a linear level spacings distribution. In the corresponding classical limit, Hamiltonians generically possess a characteristic structure of regular and stochastic orbits in phase space. Only certain simple Hamiltonians can avoid these generic features. These generic features had never before been incorporated into a calculation of relaxation. The coupling model attempts to do just that. The interest in doing this is that any realistic complex system such as a glass will almost certainly have these generic features. Such complex systems do not exhibit the simple exponential decay eq 2.2, so it is of interest to examine the generic case.

The original version of the coupling model incorporated the linear level spacings distribution that is generic to quantum Hamiltonians. The result was that the macroscopic variable initially decays by a constant rate $W_0 = \tau_0^{-1}$, but at times longer than a characteristic time $t_c \equiv \omega_c^{-1}$ the rate becomes explicitly time-dependent of the form $W = \tau_0^{-1}(\omega_c t)^{-n}$ where $0 < n < 1$. This is the basic result of the coupling model, and it can be summarized as

$$\begin{aligned} W(t) &= \tau_0^{-1}, \qquad \omega_c t \ll 1 \\ &= \tau_0^{-1}(\omega_c t)^{-n}, \qquad \omega_c t \gg 1 \end{aligned} \tag{2.3}$$

This result has profound consequences that will be described shortly. The model can be understood as an extension of standard treatments of relaxation that examine a Hamiltonian system coupled to a heat bath. We have recently been able to formulate the coupling model directly within the framework of relaxation developed by van Hove and Prigogine by extending the class of Hamiltonians under consideration.[32] Those studied by van Hove, Prigogine, and others were actually quite restrictive and do not possess the generic properties. If Hamiltonians with generic properties are used, then all the elements of the original coupling model emerge. In particular, this framework can be used to develop the coupling model completely on the basis of the classical equations of motion.[32]

Equation 2.3 can be understood intuitively as follows. Consider a single type of macroscopic variable, which we will refer to as a primitive species (PS), coupled to a heat bath. Most glasses, metallic glasses, and viscous liquids are known to have some residual short-range spatial order. Due to the heat bath, the PS begins to relax with a constant rate τ_0^{-1} because the molecular motions only involve the regions of short-range order. We first consider a *homogeneous* system so that all PSs have essentially the same constant rate τ_0^{-1} in each domain of short-range order throughout the material. Complex systems such as glasses do have short-range order, but they lack long-range order. Therefore, an individual PS cannot remain isolated from other PSs or other neighboring species at later times. Rather a PS is coupled via molecular, ionic, electronic, or other interactions with its complex environment that may include other PSs. Subsequent relaxation of a PS then involves sequential cooperative adjustments by both its complex environment and the PS itself. Such cooperative adjustments act to slow the simple relaxation rate τ_0^{-1} at times longer than a time $t_c \equiv \omega_c^{-1}$ that is characteristic of the cooperative adjustments. The time t_c is determined by the complex environment that has a larger spatial scale than that of the residual order. The interaction between the PS and the heat bath which is responsible for the simple relaxation rate τ_0^{-1} occurs at times short compared to t_c so that any frequency ν characteristic of the heat bath such as molecular vibrations must be larger than $\omega_c/2\pi$. The result is a time-dependent rate $W(t) = \tau_0^{-1}f(t)$, where $f(t) = 1$ for $\omega_c t \ll 1$ and $f(t) < 1$ for $\omega_c t \gg 1$. The function $f(t)$ will depend on the strength of coupling between the PS and the environment as well as the degree of complexity of the environment.

A complex environment beyond the short-range order is reflected in the dynamics by the generic properties exhibited by complex Hamiltonians. When these properties are included in a relaxation calculation, we find[1-3,32] the specific result $f(t) = (\omega_c t)^{-n}$ for $\omega_c t \gg 1$, leading to eq 2.3. Since these properties are generic, the form of eq 2.3 is not sensitive to the details of the intermolecular potentials, bond configurations, and other details of the system. It is this circumstance that allows us to avoid having to explicitly describe the molecular details. If the features that modify the relaxation rate were not generic, our approach would not be useful. Even very simple interacting polymer chain models that we have constructed exhibit these generic properties. If it were possible to construct a realistic Hamiltonian that incorporates the molecular interactions in detail, we should expect it to possess the generic properties. The specific values of τ_0, ω_c, and n do depend on such details of the material system. The parameter n ($0 < n < 1$) is a measure of the coupling strength of the PS to the complex environment. For very weak coupling to the environment, $n \cong 0$ and the rate remains nearly constant at $\omega_c t \gg 1$ (i.e., $\tau_0^{-1}(\omega_c t)^{-n} \cong \tau_0^{-1}$). However, when n is significantly greater than zero, the effect of the time-dependent rate is considerable.

Let us briefly examine the consequences of the coupling model result, eq 2.3. This describes the rate of relaxation

of the macroscopic variable

$$d\phi/dt = -W(t)\phi \tag{2.4}$$

With eq 2.3 this can be simply integrated to the result

$$\phi(t) = \phi(0)\exp(-t/\tau_0), \qquad \omega_c t \ll 1 \tag{2.5}$$

and

$$\phi(t) = \phi(0)\exp\left[-\int_0^t dt'\,\tau_0^{-1}(\omega_c t')^{-n}\right] \qquad \omega_c t \gg 1 \tag{2.6}$$

The slower than exponential decay eq 2.6 reflects the coupling of the PS to its complex environment. We have been able to determine[2-3,33] ω_c for some polymers, and it is typically in the range $\omega_c \cong 10^9$–10^{10} s^{-1}. Equation 2.6 will be applied to volume recovery in the next section. The material-dependent parameters τ_0, ω_c, and n may change during the course of structural recovery. However, the case of structural equilibrium is simpler and gives much insight into the meaning of eq 2.6. If τ_0, ω_c, and n are constant on the time scale of a relaxation experiment, eq 2.6 can be further simplified as

$$\phi(t) = \phi(0)\exp[-t^{1-n}/((1-n)\omega_c{}^n\tau_0)] \tag{2.7}$$

or

$$\phi(t) = \phi(0)\exp[-(t/\tau^*)^{1-n}], \qquad \omega_c t \gg 1 \tag{2.8}$$

$$\tau^* \equiv [(1-n)\omega_c{}^n\tau_0]^{1/(1-n)} \tag{2.9}$$

In this situation we immediately obtain the fractional exponential or Kohlrausch decay function[3] which is commonly observed in relaxation experiments (e.g., see eq 1.8). The effective relaxation time τ^* of the complex system has been defined, and it is related to the primitive relaxation time τ_0 by eq 2.9. Notice that eq 2.8 and 2.9 both contain the same parameter n. The measured relaxation time τ^* is thus related to the shape of the time decay function. This leads immediately to testable predictions because eq 2.8 and 2.9 must both be obeyed for the same value of n. If relaxation data conforms to the Kohlrausch form, n can be determined by comparing eq 2.8 to the data. This value of n can then be used in eq 2.9 to predict properties of τ^*. For example, suppose it were known from experiments or theory that the relaxation time for the PS had certain dependences on, e.g., molecular weight, temperature, pressure, or other variables

$$\tau_0 = \tau_0(M,T,P,...) \tag{2.10}$$

Then eq 2.9 predicts

$$\tau^* \propto [\tau_0(M,T,P,...)]^{1/(1-n)} \tag{2.11}$$

This type of prediction has been repeatedly verified for several different relaxation processes and many different materials. A good example is the terminal relaxation in polymer melts.[2,34-37] For low molecular weight, $M < M_c$, the linear chains can be considered uncoupled, and this represents the PS. It is known that $G \sim \exp(-t/\tau_0)$ and $\tau_0(M,T) \sim M^2\zeta_0(T)$, where $\zeta_0(T)$ is the simple friction factor. In polyethylene, $\zeta_0(T) \sim \exp(E_a/RT)$ where the rotational isomerism barrier $E_a = 3.6$ kcal/mol has been measured spectroscopically.[35] If $M > M_c$, the chains are entangled and coupled, i.e., the PS is coupled to a complex environment. The terminal relaxation modulus of monodisperse entangled polyethylene melts is described well[34-35] by eq 2.8 with $n \cong 0.41$. Monodisperse melts have chains of nearly the same molecular weight. The τ_0 will then be essentially the same for each chain (i.e., homogeneous system). Since both n and $\tau_0(M,T)$ are known from measurements, we can predict $\tau^*(M,T)$ with eq 2.9 or eq 2.11: $\tau^* \sim M^{2/(1-n)}\exp(E_a/(1-n)RT) \sim M^{3.4}\exp[(6.35\ \text{kcal/mol})/RT]$, in agreement with measurements on monodisperse entangled polyethylene melts.[35] Thus the coupling model successfully predicts the results of rheological measurements from molecular properties.

The coupling model does not present a theory for either τ_0 or τ^*, but it is able to predict relations between these two relaxation times. Other examples where eq 2.8 and 2.9 have been simultaneously verified include several different phenomena in primary and secondary relaxations in polymers, ionic conductivity relaxations, and electronic hopping conductivity relaxations.[1-3] The coupling model not only predicts Kohlrausch decay based on fundamental properties of dynamical systems but also provides a physical criterion for its appearance. The criterion is that, as mentioned above, the system is homogeneous so that all PSs have the same τ_0 throughout the material. If the system is inhomogeneous, there can be several primitive relaxation times τ_{0_1}, τ_{0_2}, ... The generic properties of Hamiltonians will now modify each of these primitive relaxations so that the complex system is described by a combination of several Kohlrausch functions with n_1, n_2, ... In the polymer-melt example, homogeneous systems with all chains nearly the same length (i.e., monodisperse) can be accurately made by chemists. Indeed, the terminal region of polydisperse polymer melts deviates considerably from a single Kohlrausch decay.[3] The inhomogeneous situation is more difficult to test. It is interesting that many condensed matter systems can be described by a *single* primitive τ_0 and the coupling model.

The coupling model predicts a nonexponential Kohlrausch decay in complex systems even for a single primitive τ_0. Most work in polymers and glasses assumes a single exponential corresponding to each relaxation time i.e., eq 2.2. The effects of complexity are often attributed to the existence of many different τ's. This is assumed in the KAHR and Robertson models. However, as described above, a single-exponential decay has been justified from the equations of motion only for simple systems. The modification of the rate equation by the generic properties of dynamical systems represents genuinely new physics. The Kohlrausch decay eq 2.8 predicted by the coupling model is not equivalent to a weighted sum of exponentials because of the simultaneous prediction between τ^* and τ_0 in eq 2.9. If we write $\phi(t) = \phi(0)\sum g_i\exp(-t/\tau_i)$, it is possible to carefully choose the distribution of relaxation times $g_i(\tau_i)$ so that it equals a Kohlrausch function $\exp[-(t/\tau)^{1-n}]$ for some n. However, eq 2.9 *cannot* be produced by such a distribution. If each τ_i is proportional to a basic relaxation τ_0, $\tau_i = \tau_0 a_i$, then it is easy to show that $\tau \propto \tau_0$. This is in contrast to $\tau^* \propto \tau_0{}^{1/(1-n)}$ from the coupling model. Thus the physical situations analyzed by the coupling model cannot be described by a distribution of relaxation times alone.

Moynihan's model uses a nonexponential function with a single relaxation time. However, this was proposed as a generalization of the Kohlrausch function, and it was not derived. The coupling model result eq 2.6 also generalizes Kohlrausch to situations of structural recovery, but it is based on generic properties of dynamical systems. Moynihan's phenomenological expression eq 1.10 is not the same as the coupling model result eq 2.6, and its implications for volume recovery are quite different. This will be shown clearly in the next section.

Although eq 2.8 and 2.9 have been tested repeatedly, the general result eq 2.6 has not been quantitatively tested. Limited simulations were previously presented,[38] but no predictions were tested. The general result requires not

just single values of τ_0, ω_c, and n but their functional dependences on structure. However, sufficient data is available for application to volume recovery in PVAc. The explicitly time-dependent rate of the coupling model arises from fundamental properties of complex dynamic systems and should be incorporated into any model of structural recovery. These physical features are not considered in previous models, and from our viewpoint, this omission must lead to deviations from experimentally observed behavior.

3. Coupling Model Predictions in Volume Recovery

The basic result of the coupling model is the time-dependent rate $W(t)$ eq 2.3 in which a constant primitive rate τ_0^{-1} is modified at long times ($\omega_c t \gg 1$) by the time-dependent factor $(\omega_c t)^{-n}$ due to coupling with the complex environment. This determines the properties of relaxation. In structural equilibrium, it leads to the Kohlrausch decay eq 2.8 and the relation eq 2.9 between τ_0 and the measured relaxation time τ^*. These predictions have been repeatedly verified. The time-dependent rate should also determine the features of structural recovery. Most of our discussion of volume recovery will be in terms of the directly observable parameters n and τ^*. We will later discuss the predicted behavior of τ_0 using eq 2.9. Therefore, it will be useful to rewrite $W(t)$ in eq 2.3 directly in terms of τ^* by using eq 2.9 to eliminate $\omega_c{}^n\tau_0$

$$W(t) = (1-n)\tau^{*-1}(t/\tau^*)^{-n}, \qquad \omega_c t \gg 1 \tag{3.1}$$

In structural equilibrium, n was the fractional exponent of the Kohlrausch function, and it determined the shape of the relaxation spectrum. The value of n depends both on the material and the relaxation process under consideration. During structural recovery, it is possible for n to change with the structure. There is evidence for changes in the shape of the relaxation spectrum in PVAc during volume recovery. Kovacs, Stratton, and Ferry (KSF)[39] studied the dynamic storage and loss shear moduli over a range of frequencies as a function of elapsed time after quench from a temperature well above T_g to several temperatures near T_g ($T_g \cong 33$ °C). Volume contraction measurements were also made on the same samples under essentially the same conditions. The method of reduced variables was applied to the frequency dependence of G' and G'' at various temperatures by using shift factors. The shift factors are considered as functions of temperature and the elapsed time after quench $a(T,t)$ or, alternately, as functions of temperature and the volume deviation $a(T,\delta)$. They were calculated by KSF by using a modified Doolittle equation with a reference state of volume equilibrium at 35 °C

$$\log a(T,\delta) = (1/2.303)(1/f(T,\delta) - 1/f(35,0)) \tag{3.2}$$

where

$$f(T,\delta) = f(35,0) + \alpha_f(T-35) + \delta \tag{3.3}$$

Here δ are the measured volume deviations corresponding to the same thermal history. KSF found that the values $f(35,0) = 0.0225$ and $\alpha_f = 5.3 \times 10^{-4}$ K^{-1} give the correct temperature dependence of the shift factors in volume equilibrium ($\delta = 0$). If δ is considered as a measure of the deviation of a fictive temperature T_f from the actual temperature T, then

$$\delta = \Delta\alpha(T_f - T) \tag{3.4}$$

Here $\Delta\alpha$ is the excess expansion coefficient of the liquid with respect to the glass as mentioned in section 1. KSF estimate $\Delta\alpha \cong 4.4 \times 10^{-4}$ K^{-1} for their samples, and this is not identical with α_f. For G', which is negligibly affected by changes in the shape of the relaxation spectrum, the shift factor eq 3.2 was successful in putting all the data on a single composite curve. Equation 3.2 was also tested for G' during volume expansion, and it agreed with a shift factor determined empirically from the data. These shifts correspond to progressive increases in the relaxation time as volume recovery proceeds. Since the T and δ dependence of the shift factors are identical for shear and volume deformation near T_g, KSF concluded that the corresponding molecular motions are similar. They found, however, that the G'' data at various temperatures and elapsed time after quench (or δ) did not reduce satisfactorily at long elapsed times and low temperatures (i.e., corresponding to $f(T,\delta) < 0.022$ in eq 3.3).

This was analogous to the lack of superposition which KSF found at volume equilibrium for $T \leq 33$ °C. These results indicate a change in the shape of the relaxation spectrum as $\delta \to 0$ and as T decreases. In the coupling model, this would correspond to a change in n as $\delta \to 0$ and as T decreases. Although KSF did not fit their volume equilibrium data to a Kohlrausch function eq 2.8 to determine n, the Kohlrausch function has been found to accurately describe the primary relaxation near T_g in many polymers. The KSF G'' measurements extend over only about $1^1/_2$ decades at each temperature, and this does not permit an accurate determination of n. Plazek has measured torsional creep compliance in polystyrene below T_g at a series of aging times.[40] If the relaxation modulus is described by $G(t) = G_0 \exp[-(t/\tau^*)^{1-n}]$ (i.e., Kohlrausch function, eq 2.8), then the corresponding compliance $J(t)$ can be obtained by numerically solving the convolution relation

$$t = \int_0^t d\tau\, J(\tau)G(t-\tau) \tag{3.5}$$

Plazek, Ngai, and Rendell solved eq 3.5 for $J(t)$ and fit it to the measured compliances to determine n at each aging time.[40] These fit the measured $J(t)$ very well, and the results were consistent with an increase of n with aging times. This is similar to the KSF results in PVAc. For polystyrene, n increased with aging from 0.55 to 0.66. Furthermore, the observed increase in τ^* was found to follow the second coupling model prediction eq 2.9 as physical aging proceeded. Shear creep measurements were also obtained by Plazek[28] in PVAc in the softening transition region, $T \simeq 37.5$–60 °C. The short-time response in the range $37.5 \leq T \lesssim 40$ °C is governed by the primary relaxation. Ngai and Plazek[41] have found that $J(t)$ in this range is also accurately described by eq 3.5 with $G(t)$ given by a Kohlrausch function. Their fits were consistent with a constant value of n in the range $0.55 \leq n_\alpha \leq 0.59$. For these temperatures the compliances can be reduced to a single composite curve, and Plazek found that his shift factors $a(T)$ are in agreement with the KSF shift factors at $\delta = 0$. In making this comparison, Plazek adjusted the KSF shift factor to account for the different moisture content in the Plazek and KSF samples.[28] We also note that dielectric measurements in PVAc are well described by the Kohlrausch function.[26,42] The value of n is found to increase as T decreases.

Therefore, we should allow for the possibility of n changing the structure and temperature. The dependence of n on the detailed molecular structure is quite complicated. However, a simple way to label these changes in n is to consider it as a function of T and δ, $n = n(T,\delta)$, or equivalently as a function of T_f using eq 3.4, $n = n(T_f)$. The observed relaxation time can be labeled in a similar way, $\tau^* = \tau^*(T,\delta)$. For volume recovery the macroscopic

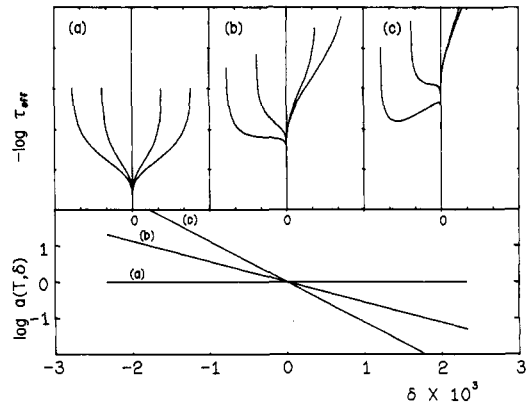

Figure 3. Calculation of τ_{eff} using coupling model (eq 3.6–3.8) with $n = 0.5$, $\tau^*(35,0) = 0.14$ h, and $\Delta\alpha = 4.65 \times 10^{-4}$ K^{-1}. As the dependence of $a(T,\delta)$ on δ becomes stronger, asymmetry and an expansion gap are produced.

variable ϕ, discussed in section 2, is identified with δ. Then the time-dependent rate eq 3.1 determines the relaxation of the volume recovery

$$\delta(t) = \delta_0 \exp\left[-\int_0^t dt' (1-n)\tau^{*-1}(t'/\tau^*)^{-n}\right] \quad (3.6)$$

Here the rate parameters $n = n(T,\delta(t'))$ and $\tau^* = \tau^*(T,\delta(t'))$ evolve as the volume recovery proceeds. This is equivalent to eq 2.6 with $\omega_c{}^n\tau_0$ eliminated by use of eq 2.9. Note that since both n and τ^* appear inside the integral in eq 3.6, the history-dependent change of both these parameters is an inherent property of the coupling model. The solution of eq 3.6 must be done self-consistently in δ. Equation 3.6 assumes a single instantaneous T jump from T_0 to T_1, causing an initial deviation $\delta_0 = \Delta\alpha(T_0 - T_1)$. This corresponds to $T_f = T_0$ at $t = 0$ in eq 3.4. Equation 3.6 also assumes that the underlying primitive relaxation time τ_0 is homogeneous throughout the material and is common to all the primitive species. An inhomogeneous situation would be described by a series of terms of the form eq 3.6. Each term could have a different τ^* and n: τ_1^*, τ_2^*, etc., and n_1, n_2, etc. Since the coupling model with homogeneous τ_0 accurately describes many volume equilibrium experiments, we will first examine the volume recovery data using eq 3.6.

Given the functional dependences $n(T,\delta)$ and $\tau^*(T,\delta)$, eq 3.6 is solved numerically by an iterative procedure. Let us define the τ^* dependences in terms of a shift factor with a reference state of volume equilibrium at 35 °C.

$$a(T,\delta) \equiv \tau^*(T,\delta)/\tau^*(35,0) \quad (3.7)$$

This will allow us to compare the results of our analysis with the KSF shift factor measurements as described by their Doolittle equation, eq 3.2. Using the definition in eq 1.2, we can also obtain an expression for τ_{eff} within the coupling model

$$\tau_{eff}^{-1} = (1-n)\tau^{*-1}(t/\tau^*)^{-n} \quad (3.8)$$

This is precisely the time-dependent rate $W(t)$ in eq 3.1. The value of δ in $n(T,\delta)$ and $\tau^*(T,\delta)$ corresponding to the time t must, of course, be taken from the self-consistent solution of eq 3.6. Before examining the volume recovery data, let us explore the general properties of eq 3.6 and 3.8.

For simplicity, first consider n to be constant. At $T = T_1 = 35$ °C and $n = 0.5$, we have calculated $\delta(t)$ for several $a(T,\delta)$ dependences on δ. The initial value of δ is given by $\delta_0 = \Delta\alpha(T_0 - T_1)$. We have used $\Delta\alpha = 4.65 \times 10^{-4}$ K^{-1}, which is compatible with the values reported by Kovacs.

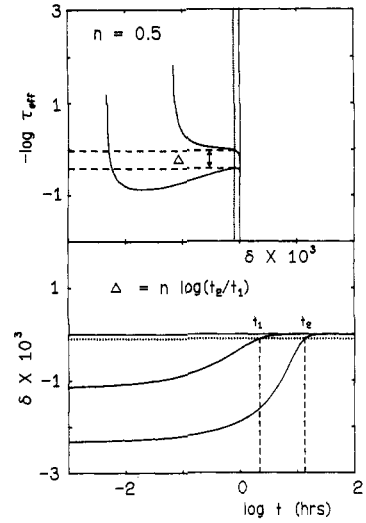

Figure 4. Illustration of the coupling model expansion gap relation, eq 3.9, using Figure 3c. Given $R = t_2/t_1$, the gap is a direct measure of n.

Figure 3 shows the corresponding calculated τ_{eff} plots. Figure 3a shows the result for $a(T,\delta) =$ constant. This is completely symmetrical in the expansion and contraction curves. However, Figure 3b shows that a decrease in $a(T,\delta)$ with δ results in a substantial asymmetry, and the results for both expansion and contraction are similar to the data (e.g., Figure 1). The approach of the expansion curves flatten as they approach $\delta = 0$. In particular, a gap has now appeared between the expansion curves near $\delta = 0$. Thus, the coupling model readily produces the expansion gap. Figure 3c shows that a faster decrease of $a(T,\delta)$ with δ results in a steeper approach of the expansion curve to $\delta = 0$ with positive slope and an enhancement in the size of the gap. The gap persists for very small δ. However, the curves eventually do merge at $\delta = 0$.

These results can be easily understood, and they are a direct result of the time-dependent rate $W(t)$, eq 3.1, predicted by the coupling model. As mentioned, this is identical with τ_{eff}^{-1} in eq 3.8. For a given value of $\delta = \delta' \cong 0$, the values of log τ_{eff}^{-1} corresponding to $T_0 = T_{0a}$ and $T_0 = T_{0b}$ differ by a substantial amount. From eq 3.8 this difference, the gap Δ, is simply

$$\Delta \equiv \log \tau_{eff}^{-1}(T_{0a},\delta') - \log \tau_{eff}^{-1}(T_{0b},\delta') = n \log [t_{\delta'}(\mathbf{b})/t_{\delta'}(\mathbf{a})] \quad (3.9)$$

Here $t_{\delta'}(\mathbf{a})$ and $t_{\delta'}(\mathbf{b})$ are the times at which the value $\delta = \delta'$ is reached corresponding to T_{0a} and T_{0b}, respectively. For a given value of the ratio $R \equiv t_\delta(\mathbf{b})/t_{\delta'}(\mathbf{a})$, the size of the gap is a direct measure of n. Consider the expansion curves in Figure 3c in more detail. This is replotted in Figure 4 along with the corresponding $\delta(t)$ vs. log t curves. From the plots we find that log $t_{\delta'}(32.5\ °C) \cong 1.13$ and log $t_{\delta'}(30\ °C) \cong 0.34$ at $\delta' \times 10^3 = -0.1$. They are about 0.79 decades apart, and therefore $R = 10^{0.79}$. The size of the gap should then be $\Delta = n \log R = 0.5 \times 0.79 = 0.4$ decade. This gap size is verified directly from the τ_{eff} plots. The gap in Figure 4 is sizable because n is significantly different from zero and because R is significantly greater than one. The value of R is history dependent and is a function of T_{0a}, T_{0b}, and $a(T,\delta)$. However, for a given value of R, the gap size gives a direct measure of the coupling parameter n. This is demonstrated in Figure 5 where τ_{eff} plots have been calculated for $n = 0.3$, 0.5, and 0.7. A different $a(T,\delta)$ has been used in each case, and it has been adjusted so that R is the same for all three cases (i.e., $R = 10^{1.3}$ at $\delta' \times 10^3 = -0.1$). Note that the shapes of the τ_{eff} curves must be

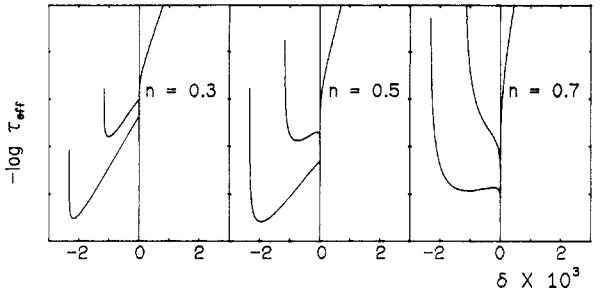

Figure 5. Illustration of the coupling model expansion gap relation, eq 3.9 for fixed $R = t_2/t_1 = 10^{1.3}$. The gap size increases in proportion to n.

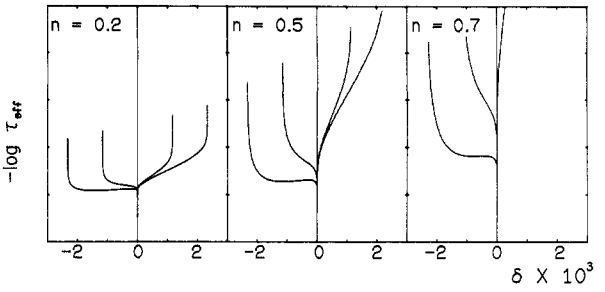

Figure 6. Illustration of the coupling model expansion gap relation, eq 3.9. For each n, $a(T,\delta)$ was adjusted to produce the same slope for the $T = 30$ °C curves as $\delta = 0$ is approached. The gap size can then be tuned by increasing n.

quite different in order to produce the same R in each case. The gap size indeed increases in proportion to n in Figure 5. As we shall see, eq 3.9 is quantitatively verified in the data.

In contrast to this, Figure 3a did not have a gap even though $n = 0.5$. The reason for this is that $R = 10^{0.22}$ here and, therefore, $\Delta = 0.5 \times 0.22 = 0.11$. R is significantly greater than 1 only if $a(T,\delta)$ changes with δ. With eq 3.6 and 3.8, the slope S on the τ_{eff} plot takes the form

$$S \equiv \frac{\mathrm{d}}{\mathrm{d}\delta}[-\log \tau_{\text{eff}}] = \left[\frac{n}{(1-n)(t/\tau^*)^{1-n_\delta}}\right] + \left[-(1-n)\frac{\mathrm{d}\log \tau^*}{\mathrm{d}\delta}\right] \equiv S_1 + S_2 \tag{3.10}$$

Term S_1 has its origin in the explicit t dependence in $W(t)$ while S_2 arises from the change of τ^* with δ. Note that $S_1 < 0$ for expansion and $S_1 > 0$ for contraction while $S_2 \geq 0$ always. Thus if $\tau^*(T,\delta)$ (or $a(T,\delta)$) has significant variation with δ, then S_1 and S_2 have opposite signs in expansion, and they compete. At both early times and long times (i.e., $\delta \cong 0$), S_1 dominates. At intermediate times, S_2 contributes and produces the flattening or even positive slope in the expansion τ_{eff} plots. S_2 contributes over a larger range of δ in the $T_0 = 30$ °C curve than the 32.5 °C curve in Figure 3c (or Figure 4). This allows $t_{\delta'}(30\ °C)$ to be significantly larger than $t_{\delta'}(32.5\ °C)$ and thus $R \gg 1$. In Figure 3a, $S_2 = 0$, and this results in $R \cong 1$. Notice that in contraction, S_1 and S_2 have the *same* sign. Therefore, $R \cong 1$ and no gap behavior is ever seen in contraction.

Figure 5 illustrates that for a given value of R, the size of the gap is determined by n while the shapes of the τ_{eff} curves are quite different for different n. It is also true that for a given shape of the τ_{eff} curves, the size of the gap is determined by n. This is demonstrated in Figure 6 for $n = 0.2$, 0.5, and 0.7. In each case, $a(T,\delta)$ was adjusted so that the slope of the $T_0 = 30$ °C curves are about the same as they approach $\delta = 0$ (i.e., similar to Figure 1). The size of the gap is then seen to increase with n. The values of R are quite different in these three cases. Figure 6 is thus complementary to Figure 5. The property illustrated in Figure 6 will allow us to fit the shape of the τ_{eff} expansion data in Figure 1 by adjusting $a(T,\delta)$ and to fit the gap size by tuning the n value.

The coupling model thus predicts that the expansion gap is a direct consequence of a structural-dependent relaxation time and a broad relaxation spectrum as measured by n. However, this is not true of the previous phenomenological models even though they contain these elements. The expansion gap predicted from Moynihan's expression eq 1.10 is

$$\Delta_{\text{M}} = (1-\beta)\log\left[\int_0^{t(\mathbf{b})} \mathrm{d}t'\tau^{-1} \Big/ \int_0^{t(\mathbf{a})} \mathrm{d}t'\,\tau^{-1}\right] \tag{3.11}$$

Whereas the coupling model prediction eq 3.9 depended on the ratio of $t_\delta(\mathbf{b})$ and $t_\delta(\mathbf{a})$, the Moynihan gap depends on the ratio of the integrals of τ^{-1} over all previous times. The ratio of these integrals is smaller than the ratio of the times $t_\delta(\mathbf{b})/t_\delta(\mathbf{a})$. In the calculation of Moynihan's function in Figure 2, we find that $t_{\delta'}(30)$ and $t_{\delta'}(32.5)$ are 0.4 decades apart at $\delta' \times 10^3 = -0.1$ while the ratio of the integrals is only $10^{0.24}$. Thus $\Delta_{\text{M}} = 0.5 \times 0.24 = 0.12$ by eq 3.11 for Moynihan's expression. No significant gap appears regardless of what value of β or variation of $\tau(T,\delta)$ is used. The expansion gap from the KAHR model also depends on the integrals over τ^{-1} up to $t_{\delta'}(\mathbf{b})$ and $t_{\delta'}(\mathbf{a})$, although in a more complicated way. The absence of a gap in the KAHR model may have a similar origin to that of Moynihan's.

The coupling model predicts that the gap $\Delta = n \log R$ observed during structural expansion recovery has the same origin as the relations $G(t) = G_0 \exp[-(t/\tau^*)^{1-n}]$ and $\tau^* = [(1-n)\omega_c{}^n\tau_0]^{1/(1-n)}$ observed at structural equilibrium. Therefore, if R is read from the measured δ vs. log t recovery curves and the size of the gap Δ is found from the corresponding τ_{eff} plot, the value of n can be predicted. This should equal the n found from fitting equilibrium relaxation data to the Kohlrausch function.

Let us now quantitatively examine the volume recovery data. We will begin with expansion data because of the importance of the expansion gap. Consider the $T_1 = 35$ °C expansion curves with $T_0 = 30$ and 32.5 °C in Figure 1. After the temperature jump from T_1 to T_0, the volume deviation begins at the value $\delta_0 = \Delta\alpha(T_0 - T_1)$ and recovers to $\delta = 0$. From estimates of the values of δ_0 from Figure 1 we find $\Delta\alpha = 4.65 \times 10^{-4}$ K^{-1}. This is consistent with the measured value of $\Delta\alpha$ reported by Kovacs. Experimentally, $\Delta\alpha$ has only a slight dependence on temperature and on the time after quench, and we will assume the constant value $\Delta\alpha = 4.65 \times 10^{-4}$ K^{-1} in all the following calculations. The $a(T,\delta)$ dependence on δ determines the shape of the τ_{eff} curves while n determines the size of the gap as is illustrated in Figure 6. This allows us to determine n and $a(T,\delta)$ almost uniquely. Figure 7 shows a comparison of calculated τ_{eff} curves with the data. These curves were calculated with $n = 0.55$. If n is constant, we have found that it must be in the range $0.55 \leq n < 0.57$ to be consistent with the observed gap. A comparable fit can also be obtained with n changing self-consistently as a function of δ (or T_f). A linearly decreasing $n(T_f)$ from $n(T_f) = 0.58$ at $T_f = 30$ °C to $n(T_f) = 0.53$ at $T_f = 35$ °C produces virtually the same result as Figure 7. Therefore, it is consistent with a slight change in the shape of the spectrum as reported by KSF. If n is allowed to change over a larger range, the gap size becomes unacceptably large. The $a(35,\delta)$ function which is required by the shape of the τ_{eff} plots is also shown in Figure 7. The value of $\tau^*(35,0)$ must be specified to determine the magnitude of

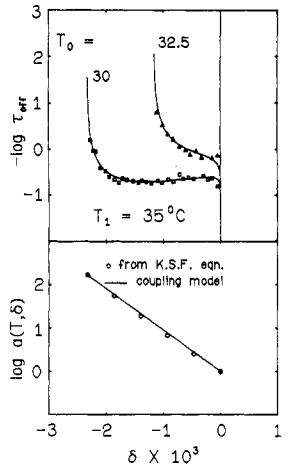

Figure 7. Comparison of the coupling model with expansion data of Figure 1 at 35 °C. Here $\tau^*(35,0) = 0.14$ h, $\Delta\alpha = 4.65 \times 10^{-4}$ K^{-1}, and $n = 0.55$. The value $n = 0.55$ agrees with measurements of Plazek in equilibrium and the predicted shift factor $a(T,\delta)$ agrees with the independently measured KSF shift factor, eq 3.2.

τ^* (e.g., see eq 3.7). We have found that $\tau^*(35,0) = 0.14$ h shifts the curves into the experimental time window.

Therefore, the coupling model is consistent with the $T = 35$ °C expansion data only for a very narrow range of the coupling model parameters. Let us examine the implications of these results. The range $0.55 \leq n < 0.57$ of constant n found from the volume fits is compatible with the range of $0.55 \leq n_\alpha \leq 0.59$ found by Ngai and Plazek[41] by relating the Kohlrausch function to shear creep compliance data on PVAc at temperatures 37.5 °C $\leq n <$ 40 °C. The Plazek samples were drier than the Kovacs samples. It is then possible that the Kovacs samples used in the volume recovery have smaller n values. We have found on other occasions that plasticizers (e.g., moisture) may cause a slight decrease in n. The n's from the volume and the shear creep found here, however, are consistent. This is in accord with the coupling model interpretation of the expansion gap described above. The same functional dependence of $a(35,\delta)$ on δ is used to generate both the $T_0 = 30$ and 32.5 °C curves in Figure 7. In Figure 7, this is compared with the shift factor measured independently by KSF and represented by their Doolittle equation, eq 3.2. Our predicted shift factor is essentially identical with the KSF shift factor. Using a different value of n within the allowed ranges discussed above produced the same agreement with the KSF shift factor. We have found a systematic correlation between the quality of fit of the calculated τ_{eff} curves to the data and the agreement between the calculated and KSF shift factors. For instance, if we use an n that is too small to produce the gap (e.g., $n = 0.5$ instead of $n = 0.55$), then the calculated shift factor deviates from the KSF shift factor. The close fit of the τ_{eff} curves to the data in Figure 7, including the gap, corresponds to a close agreement between the shift factors. This detailed reproduction of the τ_{eff} expansion curves using a $\Delta\alpha$ value as reported by Kovacs and independently measured n and $a(35,\delta)$ provides strong support for the coupling model. The only other parameter used was $\tau^*(35,0) = 0.14$ h. We do not have an independent measurement of this, but the value is quite reasonable when compared to the time scale in the δ vs. log t data in Figure 1.

For the $T_0 = 30$ °C and $T_1 = 35$ °C curve, the fictive temperature from eq 3.4 changed from $T_f = 30$ °C to $T_f = 35$ °C as δ recovered from δ_0 to 0. The value of $n(T_f)$ remained constant at 0.55 in Figure 7 as T_f changed from 30 to 35 °C although, as discussed, comparable fits could

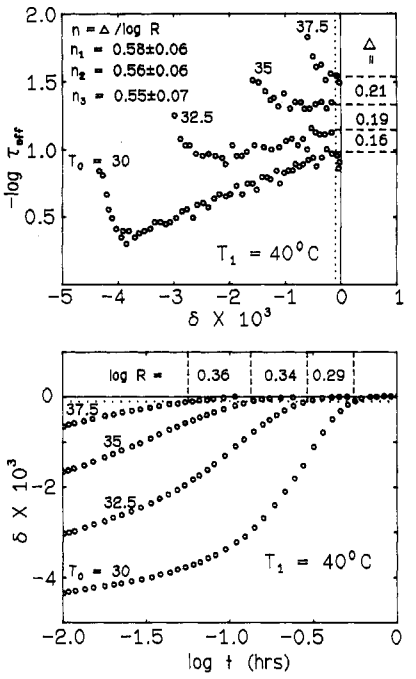

Figure 8. Volume recovery data of Kovacs (ref 5) in PVAc at 40 °C. For each pair of curves, Δ and $R = t_2/t_1$ are estimated and a value of n is obtained from the expansion gap relation, eq 3.9. These are consistent with measurements of Plazek in equilibrium.

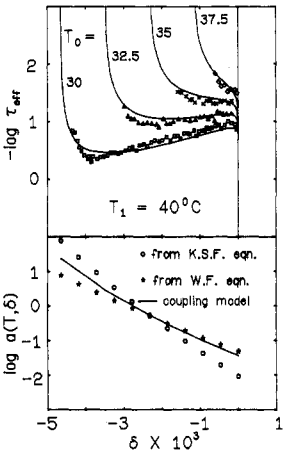

Figure 9. Comparison of the coupling model with expansion data of Figure 8 at 40 °C. Here $\tau^*(35,0) = 0.14$ h, $\Delta\alpha = 4.65 \times 10^{-4}$ K^{-1}, and n is given by eq 3.12. The n values are consistent with measurements of Plazek in equilibrium and the predicted shift factor follows the modified WF Doolittle equation as $\delta \rightarrow 0$.

be obtained in which n changed by $\Delta n \cong 0.05$. Let us now examine the expansion data at $T_1 = 40$ °C. The δ vs. log t data and corresponding τ_{eff} plots are shown in Figure 8. Now T_f will change from 30 to 40 °C when the initial temperature is $T_0 = 30$ °C. To be compatible with the $T_1 = 35$ °C calculation in Figure 7, $n(T_f)$ should be constant at 0.55 at least between $T_f = 30$ °C and $T_f = 35$ °C. The simplest continuation between $T_f = 35$ °C and $T_f = 40$ °C would be for $n(T_f)$ to remain constant at 0.55. Using $n = 0.55$ constant, we have calculated the $T_1 = 40$ °C expansion curves for $T_0 = 30$, 32.5, 35, and 37.5. The $a(40,\delta)$ dependence on δ is determined by obtaining the best fit to all four curves. The results are able to reproduce both the shape of the τ_{eff} curves and the size of the gaps between each pair of curves near $\delta = 0$. However, we have found that a slight decrease in n between $T_f = 35$ °C and $T_f = 40$ °C is able to produce a better fit to the shape of τ_{eff}

curves for T_0 = 35 °C and 37.5 °C. This calculation is shown in Figure 9 where we have used

$$n(T_f) = 0.55, \quad T_f = 30\text{–}35\ ^\circ\text{C}$$
$$= 0.55\text{–}(0.05/40)T_f, \quad T_f = 35\text{–}40 \quad (3.12)$$

A decrease in n for large T_f would be consistent with KSFs observation of a slight change in the relaxation spectrum at long elapsed times after quenching. Fits comparable to Figure 9 are obtained with $n(T_f)$ decreasing linearly from 0.58 to 0.48 between T_f = 30 and 40 °C. The gap sizes at T_1 = 40 °C are $\Delta \cong 0.2$ decade compared to $\Delta \cong 0.3$ decade at T_1 = 35 °C. The gap is smaller at T_1 = 40 °C even though n is about the same because the ratios R of times in eq 3.9 are different. In fact, we have used eq 3.9 to directly obtain the value of n from the T_1 = 40 data. This is demonstrated in Figure 8. At $\delta \times 10^3 = -0.1$, we have obtained log R between each pair of curves on the δ vs. log t plot as indicated in the figure. Similarly, we have obtained the size of the gap Δ between each pair of τ_{eff} curves. Then using $n = \Delta/(\log R)$ from eq 3.9, we find n = 0.58 ± 0.06, 0.56 ± 0.06, and 0.55 ± 0.07 from each of these estimates. This assumes an uncertainty in Δ of ±0.02 decade. These values of n agree with our self-consistent calculations for fitting the data in Figure 9. They are also in the same range as the n's obtained by Ngai and Plazek[41] by fitting shear creep compliance data on the basis of a Kohlrausch function for temperatures $37.5 \le T < 40$ °C. As mentioned earlier, it is possible that the n's for the Kovacs samples are slightly smaller than Plazek due to moisture content.

The quality of fit to the τ_{eff} curves is comparable in Figures 7 and 9 even though we have fit four curves simultaneously at T_1 = 40 °C. The function $a(40,\delta)$ determined by these fits is also shown in Figure 9. This is compared to the KSF shift factor at 40 °C as given by the Doolittle form eq 3.2. Although our $a(35,\delta)$ agreed closely with the KSF shift factor at 35 °C, our $a(40,\delta)$ is not as steep as a function of δ as KSF at 40 °C. However, KSF have pointed out that the temperature dependence of their Doolittle equation at volume equilibrium is steeper than the Doolittle equation obtained by dynamic shear measurements on PVAc at a higher range of temperature ($50 \le T \le 90$ °C) by Williams and Ferry (WF)[43] (i.e., see Figure 8 in ref 39). WF also reported that their Doolittle equation agrees with the shift factor from dielectric data ($40 \le T \le 105$ °C). When extrapolated to the range of temperatures of the KSF measurement ($T < 39$ °C), the WF Doolittle equation is not as steep as a function of T as the KSF Doolittle equation. The WF shift factor, measured at δ = 0, took the form of eq 3.2 but with the values $f(35,0)$ = 0.0298 and $\alpha_f = 5.9 \times 10^{-4}$ K^{-1}. If we follow KSFs procedure of modifying the Doolittle equation by adding δ to the fractional free volume, we can plot the modified WF shift factor as a function of δ. This WF shift factor is also compared to our $a(40,\delta)$ in Figure 9. We see that there is a close correspondence between our calculated $a(40,\delta)$ and the WF shift factor. There is some deviation near the initial δ, $\delta_0 \times 10^3 \cong -4.65$, which corresponds here to T_f = 30 °C. However, it follows the WF curve thereafter as T_f increased toward 40 °C.

Therefore, the coupling model analysis of the volume recovery predicts a shift factor $a(T,\delta)$ that at low temperatures (i.e., T_1 = 35 °C) agrees with the δ dependence of the independently measured KSF shift factor and that crosses over at higher temperatures (i.e., T_1 = 40 °C) at the WF shift factor. At T_1 = 40 °C, there is possibly an indication of a crossover from KSF at low T_f to WF at high T_f. The need to use different Doolittle or WLF equation parameters at low and high temperatures in PVAc has been verified by the more recent measurements of Plazek.[28] His shear creep compliance measurements of the softening dispersion extend from 37.5 °C to 60 °C. This overlaps both the KSF ($T < 40$ °C) and the WF ($40 \le T \le 90$ °C) temperature ranges. Plazek's samples were dry compared to the KSF and WF samples. However, Plazek showed that the temperature dependence of the shift factors from all three sets of data are compatible after correcting the T_g's of the wet samples. He concluded from his work that the PVAc data from the softening dispersion cannot be fit to any of the free volume related equations (i.e., Doolittle, WLF, etc.) over the whole temperature range 37.5–90 °C. A Doolittle equation can be used to fit a portion of this range, but different parameters must be used in different regions. Recent papers on modeling volume recovery have also discussed the limited range of WLF equations and the need to understand the temperature dependences in the different regions.[27] The coupling model is able to predict shift factors from the features of volume recovery that are compatible with existing shear data. The functional dependences of the shift factor or τ^* are predicted by the coupling model to be correlated both with the value of n and with the detailed shapes of the expansion curves. These predictions are verified in the volume expansion data.

The coupling model deals not only with the directly observable parameters τ^* and n but also relates these to a primitive relaxation time τ_0. In section 2 we gave the example of the terminal relaxation of monodisperse entangled polyethylene melts. There the molecular weight and temperature dependence of τ^* could be predicted from the molecular weight and temperature dependence of τ_0. These are related via eq 2.9 by the value of n that can be measured from $G(t)$. The temperature dependences of τ^* and τ_0 are contained in friction coefficients $\zeta(T)$ and $\zeta_0(T)$. At sufficiently high temperatures above T_g, the friction factor $\zeta(T)$ of polyethylene is thermally activated. The predicted relation $E_a^* = E_a/(1-n)$ was verified where E_a^* = 6.35 kcal/mol is the observed activation energy from flow viscosity, E_a = 3.6 kcal/mol is the rotational isomerism barrier of the molecule from spectroscopic measurements, and the measured coupling parameter is n = 0.41. A primitive τ_0 should also be responsible for the observed behavior of the volume recovery in PVAc even though it does not take a simple Arrhenius form. In fact, there is evidence that a single primitive friction coefficient $\zeta_0(T)$ governs the temperature dependence of both the primary and the terminal relaxations in PVAc. Plazek has found that the shift factor for the terminal dispersion is significantly different from that of the softening dispersion in PVAc between 37.5 and 50 °C. Ngai and Plazek[41] have been able to explain these two shift factors in terms of a common primitive friction coefficient by using the coupling model. As mentioned earlier, the n that they found for the primary relaxation contribution to the softening dispersion is in the range $0.55 < n_\alpha < 0.59$. This was consistent with our volume results. The n for the terminal dispersion, however, is in the range $0.40 < n_\eta < 0.45$. From eq 2.9, the friction coefficients are related by $\zeta_\alpha(T) \propto (\zeta_0(T))^{1/(1-n_\alpha)}$ and $\zeta_\eta(T) \propto (\zeta_0(T))^{1/(1-n_\eta)}$. In terms of the apparent activation energies defined by $E^*_{a\alpha} \equiv \partial \ln a_{T\alpha}/\partial(1/T)$ and $E^*_{a\eta} \equiv \partial \ln a_{T\eta}/\partial(1/T)$, this implies

$$E^*_{a\alpha} = \frac{E_a}{1-n_\alpha} \qquad E^*_{a\eta} = \frac{E_a}{1-n_\eta} \qquad (3.13)$$

where the primitive apparent activation energy is $E_a \equiv \partial \ln a_0/\partial(1/T)$ and $a_0 \equiv \tau_0(T)/\tau_0(T_r)$. The difference in the shift factors can be explained by the coupling model from

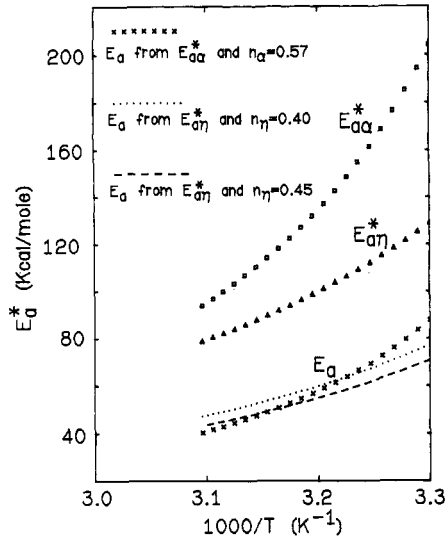

Figure 10. Effective activation energies in PVAc measured by Plazek (ref 28 and 41) for the softening dispersion $E^*_{a\alpha}$ and the terminal dispersion $E^*_{a\eta}$. $E^*_{a\alpha}$ is consistent with the shift factors of KSF and WF if adjusted for moisture content. Coupling model predicts a common primitive effective activation energy E_a, eq 3.13.

the difference between n_α and n_η. The relation $(1 - n_\alpha)E^*_{a\alpha} = (1 - n_\eta)E^*_{a\eta}$ follows from eq 3.13, and this was quantitatively verified from the measured shift factors. In Figure 10 we plot $E^*_{a\alpha}$, $E^*_{a\eta}$, and the predicted E_a as deduced from each of them by eq 3.13. As seen, the primitive $E_a(T)$ is the same for both the softening and terminal relaxations within the uncertainties in the n values.

This result has great physical appeal because the primitive friction factor should be a molecular property. $E_a(T)$ is in the range 40–80 kcal/mol, which is more reasonable for an interpretation in terms of molecular conformations than $E^*_{a\alpha}$ or $E^*_{a\eta}$. These are larger than E_a due to the cooperative effects of coupling to a complex environment. The coupling and the environment are different for the terminal and softening relaxations, and this is reflected in the different values of n_α and n_η. Theories or measurements are not presently available to directly check the $E_a(T)$ prediction. The primitive relaxation has been directly checked for the polyethylene melts and several other cases. Since Plazek has shown that $a_{T\alpha}$ is compatible with the KSF and WF shift factors, the present volume results are also consistent with the same primitive $E_a(T)$ (if we take into consideration the different moisture content of the samples). Thus, the coupling model has quantitatively linked the terminal dispersion, the softening dispersion, and the nonlinear volume recovery in terms of molecular properties. In each of these areas of polymer physics, the coupling model has been able to quantitatively resolve apparent anomalies. This reflects the fundamental origin of the time-dependent rate $W(t)$ from generic properties of dynamical systems.

Next we consider the volume recovery data in contraction. Figure 3 had illustrated that our calculated contraction curves have the correct general properties, but now we test it quantitatively. We follow the same procedure as with the expansion data. The values of $n(T_f)$ for T_f between 30 and 40 °C must be consistent with those used in Figures 7 and 9. Figure 11 shows the τ_{eff} calculations for T_1 = 30 °C with T_0 = 32.5, 35, 37.5 and 40 °C. Expansion data for T_1 = 30 °C is not available due to experimental difficulties. $a(30,\delta)$ is determined from the best fit to the shapes of the curves. The reproduction of the τ_{eff} curves is good with the exception of T_0 = 40 °C.

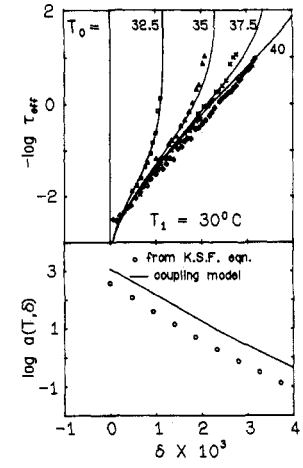

Figure 11. Comparison of the coupling model with contraction data of Kovacs (ref 5) in PVAc at 30 °C. Here $\tau^*(35,0)$ = 0.14 h, $\Delta\alpha = 4.65 \times 10^{-4}$ K^{-1}, and n is given by eq 3.12. Contraction data may involve formation of inhomogeneities following rapid cooling.

However, the overall quality of fit is not quite as good as the expansion fits in Figures 7 and 9. This is reflected in the comparison of our calculated $a(30,\delta)$ with the KSF shift factor with T = 30 °C. They have similar slope but are shifted apart in magnitude. We had noted the same systematic correspondence between quality of fit of the expansion τ_{eff} curves and agreement between shift factors. If we deliberately worsen the quality of the expansion fits, the shift factors similarly begin to deviate. The result of Figure 11 might be interpreted as evidence for the KSF shift factor in contraction if the deviations in the τ_{eff} fits can be understood. The T_0 = 40 °C curve is very close to the T_0 = 37.5 °C curve and must be considered unacceptable. Part of the reason for this may be the need for using a finite cooling ramp in the calculation for $T_0 \gtrsim 40$ °C as noted earlier by KAHR.

The discrepancies between the calculated contraction curves and the data systematically increase as we go to higher T_1. The T_1 = 35 °C contraction calculations showed unacceptable deviations even for the $\Delta T = T_1 - T_0$ = 2.5 °C and 5 °C curves, which had fit well at T_1 = 30 °C. The evidence for the coupling model in expansion must be considered quite strong. There the samples had been well aged, and the initial temperatures were below or near T_g. The contraction experiments involve rapid cooling from initial temperatures T_0, which are often several degrees above T_g. Such rapid cooling from above T_g may involve the formation of inhomogeneities within the material. If these inhomogeneities persist for a significant fraction of the volume recovery time, then our use of a primitive relaxation time τ_0 homogeneous throughout the material is no longer justified. Such inhomogeneities could not be formed during expansion. It may then be necessary to use several distinct relaxation times τ_{01}, τ_{02}, etc., for the contraction experiments. The coupling model mechanism would then generate τ_1^*, τ_2^*, etc., and n_1, n_2, etc. The dependence of each of these on T and δ may also be different. The volume recovery would then be generalized to

$$\delta(t) = \delta_0 \sum_i^N g_i \exp\left[\int_0^t dt' (1 - n_i)\tau_i^{*-1}(t'/\tau_i^*)^{-n}\right] \qquad (3.14)$$

This possibility is physically plausible and would be expected to occur only for the contraction experiments. The use of a homogeneous τ_0 would also be less applicable as T_1 and T_0 increase, and this is consistent with our

contraction calculations. However, it is difficult to quantitatively prove this at present. The $T_1 = 30$ °C results in Figure 11, where homogeneous conditions may not yet have completely broken down, can be interpreted as evidence for the role of the coupling model in contraction. However, if inhomogeneities must be accounted for in contraction by eq 3.14 for larger T_1 and T_0, then it becomes difficult to describe this in detail. Equation 3.14 contains many parameters, and it is not clear how to separate the different contributions in the data. We do not wish to use many unknown parameters to attempt a fit to contraction data. However, illustrative simulations we have run with three terms of eq 3.14 shows that this can, in principle, improve the agreement for the contraction data. At sufficiently long times into the recovery, the material may return to a homogeneous condition, and this might be possible to observe. A possible way to test this is to repeat the KSF experiment which measured shear and volume in parallel. If $G''(\omega)$ is measured over a sufficient number of decades to exhibit a loss peak, then the shape of the loss peak can be examined at different elapsed times after quench. For a homogeneous situation, the loss peak can be described by a single Kohlrausch function. The evolution of the material during contraction to a homogeneous condition might then be monitored.

4. Summary

A coupling model of relaxation has been described that predicts a time-dependent relaxation rate, eq 2.3, based on generic properties of dynamical systems. In structural equilibrium this leads to the Kohlrausch decay law eq 2.8 and a second relation eq 2.9 between the observed and primitive relaxation times. Previously, these have been repeatedly verified for several relaxation processes. The more general decay law eq 3.6 is predicted for situations out of structural equilibrium. When applied to volume recovery following a rapid temperature step, the coupling model predicts a gap in the τ_{eff} expansion data near $\delta = 0$ as observed in the experimental data. This feature could not be reproduced by any previous model. Furthermore, the coupling model is able to quantitatively relate the size of the expansion gap and the shape of the τ_{eff} plots to independently measured shift factors and relaxation functions. The size of the gap determines the value of the coupling parameter n near equilibrium. The values of n obtained from Kovacs' volume recovery data are in agreement with the Kohlrausch exponent obtained by Ngai and Plazek from shear compliance measurements in equilibrium. The shape of the τ_{eff} plots determine the δ dependence of the shift factor. The shift factor predicted from the volume recovery data are in agreement with the Doolittle equation obtained by Kovacs, Stratton, and Ferry using dynamic mechanical shear at 35 °C. The coupling model further predicts that the shift factor crosses over to the Doolittle equation of Williams and Ferry at 40 °C. The need to use different Doolittle or WLF parameters in different temperature regimes in PVAc has been emphasized by KSF, Plazek, and others.

Ngai and Plazek have previously been able to quantitatively relate the shift factors for the terminal dispersion and the softening dispersion in PVAc by use of the coupling model. The present work now relates both of these to the shift factor obtained from the volume recovery. Use of the predicted relation eq 2.9 between the observed τ^* and primitive τ_0 relaxation times shows that the same underlying τ_0 can quantitatively account for the terminal dispersion, the softening dispersion, and the volume recovery in PVAc. This represents a considerable unification of quite different relaxation regimes in a polymer.

The assumption of a single (i.e., homogeneous) relaxation time was found not to apply to the contraction data at the higher temperatures. This was consistent with the formation of inhomogeneities within the material during rapid cooling from above T_g. This situation could not be quantitatively tested with the coupling model because the several parameters involved are not presently available from independent measurements.

The coupling model is based on fundamental properties of complex dynamical systems. These properties represent genuinely new physics that have not been incorporated into previous models. The present model avoids the many phenomenological assumptions used in other models and leads to powerful predictions. The success of the coupling model in volume recovery in reproducing the expansion gap and quantitatively predicting independently measured shift factors and coupling parameters is strong evidence for the role of the coupling mechanism in structural recovery near T_g.

Acknowledgment. We thank A. J. Kovacs for his advice concerning this work and for many helpful discussions during his visits to NRL. This work was supported in part under ONR Task 4145021---02.

Registry No. PVAc, 9003-20-7.

References and Notes

(1) Ngai, K. L. *Comments Solid State Phys.* **1979**, *9*, 127; **1980**, *9*, 141.
(2) Rendell, R. W.; Ngai, K. L. In *Relaxations in Complex Systems*; Ngai, K. L., Wright, G. B., Eds.; Government Printing Office: Washington, D.C., 1985; p 309. Available from National Technical Information Service, 5285 Port Royal Road, Springfield, VA 22161.
(3) Ngai, K. L.; Rendell, R. W.; Rajagopal, A. K.; Teitler, A. *Ann. N.Y. Acad. Sci.* **1987**, 180.
(4) Kovacs, A. J. *J. Polym. Sci.* **1958**, *30*, 131.
(5) Kovacs, A. J. *Fortschr. Hochpolym.-Forsch.* **1963**, *3*, 394.
(6) Kovacs, A. J.; Aklonis, J. J.; Hutchinson, J. M.; Ramos, A. R. *J. Polym. Sci., Polym. Phys. Ed.* **1979**, *17*, 1097.
(7) Kovacs, A. J.; Hutchinson, J. M.; Aklonis, J. J. In *The Structure of Non-Crystalline Materials*; Gaskell, P. H., Ed.; Taylor and Francis: London, 1977; p 153.
(8) Aklonis, J. J.; Kovacs, A. J. *Contemp. Top. Polym. Sci.* **1979**, *3*, 267.
(9) Robertson, R. E. *J. Polym. Sci., Polym. Symp.* **1978**, *No. 63*, 173.
(10) Robertson, R. E. *J. Polym. Sci., Polym. Phys. Ed.* **1979**, *17*, 597.
(11) Robertson, R. E. *J. Appl. Phys.* **1978**, *49*, 5048.
(12) Robertson, R. E. *Ann. N.Y. Acad. Sci.* **1981**, *371*, 21.
(13) Robertson, R. E.; Simha, R.; Curro, J. G. *Macromolecules* **1984**, *17*, 911.
(14) Ngai, K. L.; Rendell, R. W., unpublished results.
(15) Moynihan, C. T.; Macedo, P. B.; Montrose, C. J.; Gupta, P. K.; DeBolt, M. A.; Dill, J. F.; Dom, B. E.; Drake, P. W.; Easteal, A. J.; Elterman, P. B.; Moeller, R. P.; Sasabe, H.; Wilder, J. A. *Ann. N.Y. Acad. Sci.* **1976**, *279*, 15 and references therein.
(16) Narayanaswamy, O. S. *J. Am. Ceram. Soc.* **1971**, *54*, 491.
(17) Hodge, I. M.; Berens, A. R. *Macromolecules* **1982**, *15*, 762. Hodge, I. M.; Huvard, G. S. *Macromolecules* **1983**, *16*, 371. Hodge, I. M. *Macromolecules* **1986**, *19*, 936.
(18) Tribone, J. J.; O'Reilly, J. M.; Greener, J. *Macromolecules* **1986**, *19*, 1732.
(19) Chow, T. S.; Prest, W. M., Jr. *J. Appl. Phys.* **1982**, *53*, 6568. Prest, W. M., Jr.; Roberts, F. J., Jr.; Hodge, I. M. *Proc. North Am. Therm. Anal. Soc. Conf., 12th* **1980**, 119–123.
(20) Kovacs, A. J. private communication.
(21) Goldstein, M.; Nakonecznyj, M. *Phys. Chem. Glasses* **1965**, *6*, 126.
(22) Roe, R. J. *Macromolecules* **1981**, *14*, 1586.
(23) Curro, J. J.; Roe, R. J. *Polymer* **1984**, *25*, 1424.
(24) Aklonis, J. J. *Polym. Eng. Sci.* **1981**, *21*, 896.
(25) Ng, D.; Aklonis, J. J. in ref 2, p 53.
(26) Sasabe, H.; Moynihan, C. *J. Polym. Sci., Polym. Phys. Ed.* **1978**, *16*, 1447.
(27) Matsuoka, S.; Williams, G.; Johnson, G. E.; Anderson, E. W.; Furukawa, T. *Macromolecules* **1985**, *18*, 2652.
(28) Plazek, D. J. *J. Polym. Sci., Polym. Phys. Ed.* **1982**, *20*, 729.

(29) Oppenheim, I., Shuler, K. E., Weiss, G. H., Eds. *Stochastic Processes in Chemical Physics: The Master Equation*: MIT Press: Cambridge, MA, 1977.
(30) Casati, G., Ed. *Chaotic Behavior in Quantum Systems, Theory and Applications*; Plenum: New York, 1985.
(31) Lichtenberg, A. J.; Lieberman, M. A. *Regular and Stochastic Motion*; Springer-Verlag: New York, 1983.
(32) Rendell, R. W.; Ngai, K. L., to be published.
(33) Ngai, K. L.; Fytas, G. *J. Polym. Sci., Polym. Phys. Ed.* **1986**, *24*, 1683.
(34) Ngai, K. L.; Rendell, R. W. *Polym. Prepr. (Am. Chem. Soc., Div. Polym. Chem.)* **1982**, *23*, 46.
(35) Ngai, K. L.; Plazek, D. J. *J. Polym. Sci., Polym. Phys. Ed.* **1985**, *23*, 2159.
(36) McKenna, G. B.; Ngai, K. L.; Plazek, D. J. *Polymer* **1985**, *26*, 1651.
(37) Rendell, R. W.; Ngai, K. L.; McKenna, G. B., to be published.
(38) Bendler, J. T.; Ngai, K. L. *Macromolecules* **1984**, *17*, 1174.
(39) Kovacs, A. J.; Stratton, R. A.; Ferry, J. D. *J. Phys. Chem.* **1963**, *67*, 152.
(40) Plazek, D. J.; Ngai, K. L.; Rendell, R. W. *Polym. Eng. Sci.* **1984**, *24*, 1111.
(41) Ngai, K. L.; Plazek, D. J. *J. Polym. Sci. Part B*: **1986**, *24*, 619.
(42) Mashimo, S.; Nozaki, R.; Yagihara, S.; Takeishi, S. *J. Chem. Phys.* **1982**, *77*, 6259.
(43) Williams, M. L.; Ferry, J. D. *J. Colloid Sci.* **1954**, *9*, 479.

Three-Phase Separation in Cyclohexane Solutions of Binary Polystyrene Mixtures

Yoshiyuki Einaga,* Yo Nakamura, and Hiroshi Fujita

Department of Macromolecular Science, Osaka University, Toyonaka, Osaka 560, Japan.
Received August 12, 1986

ABSTRACT: Three-phase separation was observed in solutions of cyclohexane and two narrow distribution samples of polystyrene with $M_w = 4.36 \times 10^4$ and 1.26×10^6 at temperatures near 14.0 °C. The phase diagram constructed from the composition data for the three phases was compared with the theoretical predictions derived from our recently proposed empirical expression for the apparent second virial coefficient Γ. A fairly good agreement was found between experiment and theory, crediting a high accuracy of our Γ function. It was also confirmed by the present calculation that three-phase separation proceeds via the heterogeneous double plait point mechanism as originally pointed out by Tompa and recently discussed in detail by Šolc and Dobashi and Nakata.

Koningsveld and co-workers[1-4] early observed three-phase separation to occur in (quasi-binary) ternary solutions consisting of diphenyl ether and two polyethylenes or cyclohexane (CH) and two polystyrenes (PS) as predicted by Tompa's theory.[5] Very recently, Dobashi and Nakata[6] published a more extensive and precise study of this phenomenon in the system of methylcyclohexane (MCH) and two narrow distribution PS. Actually, they determined the three-phase line (coexistence curve) on the temperature vs. total polymer concentration plane and compared it with the prediction from the g function (defined originally by Koningsveld and Staverman[7]) similar to that proposed by Koningsveld and Kleintjens.[8] The agreement was only moderate; the calculated curve was much narrower than the observed one and appeared 2 K below the latter. This finding is not surprising because it was already known that Koningsveld and Kleintjens' g does not take into account the dilute solution effect and the chain length dependence in the concentrated regime, as was pointed out by Nies et al.[9]

As in previous work, Dobashi and Nakata did not take direct measurements of the compositions of the three separated phases. However, experimental data of these compositions are necessary to determine the triangular phase diagram of a system containing three phases in equilibrium. They also can be used for a stringent test of a theoretical or empirical expression of the Gibbs free energy G (or the g function) of the system, since the pattern of three-phase equilibrium should be very sensitive to the form of G as a function of temperature and composition.

Motivated by these considerations we undertook an experimental study as reported in this paper. Thus, we allowed a ternary solution of cyclohexane and two narrow distribution PS to be separated into two or three phases by a suitable choice of experimental conditions and tried to measure the composition of each phase by gel permeation chromatography (GPC). Further, the results were compared with predictions from the empirical expression of G recently proposed by Einaga et al.[10] for an arbitrary mixture of monodisperse PS homologues in cyclohexane.

Proposed Expression for the Γ Function

For the ternary system considered here we designate solvent cyclohexane as component 0, shorter chain PS as component 1, and longer chain PS as component 2. We express the chemical potential μ_0 of component 0 as[10]

$$\mu_0/RT = \mu_0^\circ/RT - \phi/P_n - \Gamma(T,\phi_1,\phi_2;P_1,P_2)\phi^2 \quad (1)$$

where μ_0° is the value of μ_0 in the pure state of component 0, R the gas constant, T the absolute temperature, ϕ_i the volume fraction of component i, P_i the relative chain length of component i ($P_0 = 1$), and ϕ the total polymer volume fraction. The number-average relative chain length P_n of the polymer mixture is expressed by

$$P_n^{-1} = \sum_{i=1}^{2} \xi_i P_i^{-1} \quad (2)$$

with $\xi_i = \phi_i/\phi$, which is the weight fraction of component i in the polymer mixture subject to the usually valid assumption that the specific volume of a polymer is independent of its chain length.

From eq 1 and the Gibbs–Duhem relation it follows[10] that the chemical potential μ_i of component i ($i = 1, 2$) is given by

$$\mu_i/RT = \mu_i^\infty/RT + \ln \phi_i - \phi + (1 - P_i/P_n)\phi + \phi(1-\phi)P_i\Gamma + P_i\int_0^\phi [\Gamma + (1-\xi_i)(\partial\Gamma/\partial\xi_i)]\, d\phi \quad (3)$$

where μ_i^∞ defined by

$$\mu_i^\infty = \lim_{\phi\to 0} (\mu_i - RT \ln \phi_i) \quad (4)$$

0024-9297/87/2220-1083$01.50/0